Statistics of Optical Spectra from Single-Ring Aggregates and Its Application to LH2

Maxim V. Mostovoy and Jasper Knoester*

Institute for Theoretical Physics and Materials Science Center, University of Groningen, Nijenborgh 4, 9747 AG Groningen, The Netherlands

Received: April 20, 2000; In Final Form: August 18, 2000

We study the statistics of the optical spectra of individual ring-shaped molecular aggregates in which the site energies and transfer interactions are perturbed by both weak random disorder and a regular modulation due to a deformation of the ring. Under these conditions, the spectrum is dominated by two lines. We present an analytical expression for the joined probability distribution of the splitting between these lines and their average position. We compare our results to recent experiments performed on the bacterial antenna system LH2. Our analysis indicates the importance of intercomplex disorder.

I. Introduction

The possibility to observe single-molecule fluorescence spectra provides an entirely new view on the dynamic properties of molecular excited states, as it allows one to obtain direct information on spectral details which in ensemble averages are lost due to inhomogeneity.[1,2] When applied to molecular aggregates, this new technique opens the interesting possibility to observe directly the Frenkel exciton levels of individual aggregates. The statistical properties of the energies and polarizations of these levels give much more information on the distribution of energy and interaction disorder than can be obtained from ensemble spectra.

An important example of a molecular aggregate to which this technique has recently been applied[3−7] is the bacterial antenna complex LH2.[8] This complex contains two weakly coupled ring aggregates of 9 and 18 bacteriochlorophyll molecules (the B800 and the B850 ring, respectively).[9] In particular, the B850 ring has aroused much discussion, as it has a rather strong excitation transfer coupling between the molecules ($\sim$300 cm^{-1}),[10,11] which in principle may give rise to a large exciton delocalization size. The latter depends on the ratio between the transfer interaction and the strength of the energetic and interaction disorder within a single aggregate.[12,13] The estimates for the disorder strength vary widely and so does the exciton delocalization length, N_{del}, obtained from various types of experiments. Values of N_{del} varying from 4 to 18 molecules have been reported for the B850 ring.[14−25]

The observed single-complex spectra have recently opened new and more direct ways to obtain information on this issue. In particular, the low-temperature fluorescence excitation experiments of single LH2 complexes by Van Oijen et al.[6] have revealed interesting features. These authors observed that hidden below the broad B850 absorption peak that is seen in ensemble spectra, two narrower peaks with mutually perpendicular polarization directions occur for individual complexes (sometimes a third or even a fourth peak is observed). The splitting between the peaks varies from complex to complex and is distributed around $\sim$100 cm^{-1}. Van Oijen et al. interpreted the two peaks as originating from the optically active $k = \pm 1$ Bloch states, split by disorder and a ring deformation. Within this interpretation, they concluded that the disorder within each ring is rather small (full width at half-maximum (fwhm) = 125 cm^{-1}), leading to an almost complete delocalization of the exciton over the entire ring, and that the ring is slightly deformed into an ellipse. A similar deformation was also claimed by Hochstrasser and co-workers.[4] Van Oijen et al. enforced their claims with numerical simulations of the spectra of disordered single-ring aggregates.

In this paper, we derive analytical expressions for the distribution functions of the splitting and the mean position of the two peaks dominating the single-ring absorption spectra for rings that are not too large and weakly disordered. Our model allows for both energy and interaction disorder and for a class of ring deformations which includes ellipsoidal ones. We show that, depending on the strength of the deformation, the problem either reduces to a two-level one, where we only need to consider the mixing of the $k = \pm 1$ states, or to a three-level one, where we also need to couple the $k = 0$ state to the $k = \pm 1$ subspace. We point out that the statistics of the two dominant peaks in the experiments of ref 6 may also be understood on the basis of the three-level picture. In addition, we show that a consistent interpretation of the dominant peaks is only possible if one includes intercomplex disorder comparable in size to the typical energy spread within each complex.

The outline of this paper is as follows. In section II, we introduce the model of a ring aggregate with deformation and static disorder. We reduce this problem to a three-state Hamiltonian and we show that the stochastic properties of the various matrix elements of this reduced Hamiltonian are dominated by just one effective collective disorder strength. In section III, we diagonalize this problem for the case where a two-level reduction is justified and we determine the (joined) statistics of the level splitting and the mean position of the two resulting absorption peaks. In section IV, we compare these distributions to the experiments reported in ref 6. We also analyze these experiments in a different limit of the orginal three-state problem, where strong mixing of the $k = 0$ state into the optical states occurs. Finally, we conclude in section V, where we also discuss several open problems concerning the interpretation of the experiments.

* Corresponding author. Fax: 31-50-3634947. E-mail: knoester@phys.rug.nl.

10.1021/jp001519k CCC: $19.00
Published on Web 12/05/2000

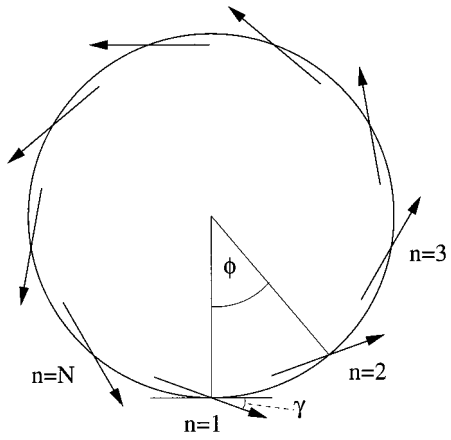

Figure 1. Ring aggregate consisting of N molecules. The arrows indicate the transition dipoles, which are equal in magnitude (d) and lie in the plane of the ring, making an angle γ with the local tangent to the ring. The angle ϕ equals $2\pi/N$.

In the Appendix we derive the coupling between the exciton states and the ring deformation for two specific deformation models.

II. Model and Reduced Hamiltonian

We consider a ring aggregate consisting of N two-level molecules placed equidistantly on a ring of radius R. The molecules are nonpolar and have identical transition dipoles of magnitude d, which lie in the plane of the ring and make an angle γ with the local tangent to the ring (Figure 1). The electronically excited states of the systems are described by a Frenkel exciton Hamiltonian that accounts for deformation of the ring and for the occurrence of energy and interaction disorder:

$$H = H_0 + H_{\mathrm{def}} + H_{\mathrm{dis}} \tag{1}$$

The unperturbed Hamiltonian reads

$$H_0 = \sum_{n=1}^{N} \omega_0 b_n^\dagger b_n + \sum_{n,m=1}^{N} J_{n,m} b_n^\dagger b_m \tag{2}$$

where $b_n^\dagger$ and b_n denote the Pauli operators[26,27] for creation and annihilation of an excitation on molecule n, respectively. Furthermore, ω_0 denotes the average transition frequency of the molecules, and $J_{n,m}$ is the excitation transfer interaction between molecules n and m. H_0 has translational symmetry along the ring, i.e., $J_{n,m}$ only depends on $n - m$ (mod(N) to account for the ring structure).

The second term in eq 1 describes the effect of a deformation of the ring. A deformation changes the intermolecular distances and thereby influences the transfer interactions. We will only account for changes in the nearest-neighbor interactions, as these are dominant. Moreover, the deformation leads to changes in the effective excitation energies of the individual molecules (in the theory of molecular excitons traditionally referred to as "crystal shifts").[26,27] Assuming the simplest modulation, which breaks the ring symmetry into a 2-fold symmetry, we have

$$H_{\mathrm{def}} = \alpha_1 \sum_{n=1}^{N} \cos(2\phi n - \Phi_1)\, b_n^\dagger b_n + \alpha_2 \sum_{n=1}^{N} \cos(2\phi(n + {}^1/_2) - \Phi_2)(b_n^\dagger b_{n+1} + b_{n+1}^\dagger b_n) \tag{3}$$

where $\phi = 2\pi/N$ and Φ_1 and Φ_2 are the phases of the two modulations, imposed by the phase of the underlying deformation along the ring. The modulation amplitudes are given by the real parameters α_1 and α_2, which reflect the exciton−lattice interaction and are proportional to the deformation amplitude. A detailed calculation of α_1 and α_2 is complicated, as it in principle also involves the (protein) environment of the ring. In particular, the calculation of α_1 requires detailed knowledge of van der Waals and quadrupolar interactions, as well as interactions with polar groups in the ring's environment. Such calculations are beyond the scope of this paper and we will keep α_1 and α_2 as general parameters (to be cast into one effective parameter α in eq 12 below). In order to make in the discussion of our results in section IV a connection between α and actual deformation amplitudes in LH2, however, we derive in the Appendix explicit expressions for α_2 for two types of ring deformations, assuming that the intermolecular (transfer) interactions are of dipolar origin. The two deformations considered are a longitudinal phonon of wavelength $N/2$ along the circumference of the ring and an ellipsoidal deformation.

Finally, the third term in eq 1 accounts for random disorder, imposed by the environment, in the molecular transition frequencies and nearest-neighbor transfer interactions:

$$H_{\mathrm{dis}} = \sum_{n=1}^{N} [\epsilon_n b_n^\dagger b_n + j_n(b_n^\dagger b_{n+1} + b_{n+1}^\dagger b_n)] \tag{4}$$

Here, the ϵ_n and j_n are independently taken from Gaussian distributions with zero means and standard deviations σ and τ, respectively:

$$\langle \epsilon_n \epsilon_m \rangle = \sigma^2 \delta_{n,m} \tag{5}$$

$$\langle j_n j_m \rangle = \tau^2 \delta_{n,m} \tag{6}$$

$$\langle \epsilon_n j_m \rangle = 0 \tag{7}$$

In the absence of disorder and modulation ($\sigma = \tau = \alpha = 0$), the one-exciton eigenstates of the Hamiltonian are Bloch states along the ring with wavenumber $k\phi$, where $k = 0, \pm 1, \pm 2, ..., \pm(N/2 - 1), N/2$:

$$|k\rangle = \frac{1}{\sqrt{N}} \sum_n \exp(ik\phi n) b_n^\dagger |g\rangle \tag{8}$$

Here, $|g\rangle$ denotes the aggregate ground state in which all molecules reside in the ground state. The pair $\pm k$ is degenerate, with energy

$$E_k = \omega_0 + \sum_m J_{n,m} \cos[(n - m)k\phi] \tag{9}$$

In the remainder of this paper, we will for explicitness assume that the dominant (nearest-neighbor) interaction is negative, implying that the $k = 0$ state lies at the bottom of the exciton band (see Figure 2).

For the circular geometry considered, with all transition dipoles in the plane of the ring, the only dipole-allowed one-exciton states are those with wavenumber $k = \pm 1$. Disorder and the ring distortion will mix the Bloch states, lifting the degeneracy within all $\pm k$ pairs and spreading oscillator strength from the $k = \pm 1$ pair to the other pairs. If the disorder strengths and the exciton−lattice interaction are small compared to the typical energy separation between different pairs ($\approx 4\pi^2|J_0|/N^2$,

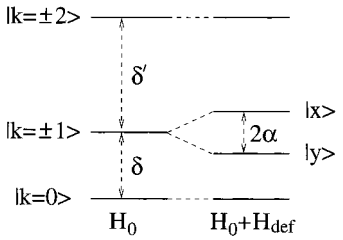

Figure 2. Low-energy level scheme of the one-exciton eigenstates of H_0 and $H_0 + H_{def}$. We have chosen a negative nearest-neighbor transfer interaction J_0 and a positive value for α. For the B850 ring in the bacterial LH2 system, $\delta \approx 66\ cm^{-1}$, while $\delta' \approx 173\ cm^{-1}$ (see section IV). The deformation-induced coupling between the $k = 0$ state and the $k = \pm 2$ states has not been taken into account in this picture.

with J_0 the nearest-neighbor interaction in the ordered ring), this spreading is small and the main effect relevant to the absorption spectrum is the mixing of the states with $k = \pm 1$. Then, it suffices to consider the Hamiltonian in the $k = \pm 1$ subspace. The applicability of this situation in the case of the B850 ring of LH2 complexes was strongly suggested by the single-complex spectra reported in ref 6. We will see later, however, that the mixing with the $k = 0$ state, which lies closest to the $k = \pm 1$ pair, may easily be too strong to justify a two-level approach. We therefore consider the Hamiltonian on the subspace of the three states $k = 0, \pm 1$. The criteria for validity of this reduction will be discussed at the end of this section.

As basis for the selected subspace we choose the three states $|0\rangle$, $|y\rangle$, and $|x\rangle$, where the last two are the real linear combinations of the complex $k = \pm 1$ states that diagonalize the deformation Hamiltonian:

$$|x\rangle = \sqrt{\frac{2}{N}} \sum_n \cos(n\phi - {}^1/_2\Phi) b_n^\dagger |g\rangle \tag{10}$$

$$|y\rangle = \sqrt{\frac{2}{N}} \sum_n \sin(n\phi - {}^1/_2\Phi) b_n^\dagger |g\rangle \tag{11}$$

Here Φ is defined by $e^{-i\Phi} = ((\alpha_1/2)e^{-i\Phi_1} + \alpha_2 e^{-i\Phi_2})/\alpha$ with

$$\alpha = \left(\frac{1}{4}\alpha_1^2 + \alpha_2^2 + \alpha_1\alpha_2 \cos(\Phi_1 - \Phi_2)\right)^{1/2} \tag{12}$$

representing half the deformation-induced splitting in the $k = \pm 1$ subspace (see below). The states $|x\rangle$ and $|y\rangle$ have transition dipoles of equal magnitude $[d(N/2)^{1/2}]$ and with mutually perpendicular orientation (arbitrarily labeled x and y).

It now is a straightforward excercise to determine the matrix elements of the total Hamiltonian on the reduced basis $|0\rangle$, $|y\rangle$, and $|x\rangle$. Setting the zero of energy at $E_{k=0}$, we arrive at the 3×3 matrix

$$H_{red} = h\mathbf{1} + \begin{pmatrix} 0 & V_y & V_x \\ V_y & \delta - \alpha - \Delta & V \\ V_x & V & \delta + \alpha + \Delta \end{pmatrix} \tag{13}$$

Here, **1** denotes the unit matrix, $\delta \equiv E_{k=1} - E_{k=0}$, while h, Δ, V, V_x, and V_y are stochastic variables defined by, respectively

$$h = \frac{1}{N} \sum_n (\epsilon_n + 2j_n) \tag{14}$$

$$\Delta = \frac{1}{N} \sum_n \{\epsilon_n \cos(2n\phi - \Phi) + 2j_n \cos[(2n+1)\phi - \Phi]\} \tag{15}$$

$$V = \frac{1}{N} \sum_n \{\epsilon_n \sin(2n\phi - \Phi) + 2j_n \sin[(2n+1)\phi - \Phi]\} \tag{16}$$

$$V_x = \frac{\sqrt{2}}{N} \sum_n \left\{ \epsilon_n \cos(n\phi - \Phi/2) + 2j_n \cos\frac{\phi}{2} \cos\left[\left(n + \frac{1}{2}\right)\phi - \frac{1}{2}\Phi\right] \right\} \tag{17}$$

$$V_y = \frac{\sqrt{2}}{N} \sum_n \left\{ \epsilon_n \sin(n\phi - \Phi/2) + 2j_n \cos\frac{\phi}{2} \sin\left[\left(n + \frac{1}{2}\right)\phi - \frac{1}{2}\Phi\right] \right\} \tag{18}$$

We note that in eq 13 we neglected contributions $(1/N)\sum_n 2j_n(\cos\phi - 1)$ on the second and third diagonal positions, which is a good approximation for rings with $N \geq 10$.

As the above collective stochastic variables are linear combinations of the underlying Gaussian random variables ϵ_n and j_n, they obey a five-dimensional Gaussian distribution $P(h,\Delta,V,V_x,V_y)$, where correlations between the five arguments cannot a priori be excluded. Using eqs 14−18 and eqs 5−7, it is straightforward to calculate the various moments of this multivariate distribution. Obviously, they all have vanishing averages. Furthermore, it turns out that in fact all five variables are mutually uncorrelated. Finally, their variances are given by

$$\langle h^2 \rangle = 2\langle \Delta^2 \rangle = 2\langle V^2 \rangle = \frac{1}{N}(\sigma^2 + 4\tau^2) \equiv D^2 \tag{19}$$

$$\langle V_x^2 \rangle = \langle V_y^2 \rangle = \frac{1}{N}\left(\sigma^2 + 4\tau^2 \cos^2\frac{\phi}{2}\right) \approx D^2 \tag{20}$$

where the last approximation again holds for rings that are not too small. We thus observe that one effective disorder parameter D suffices to describe the stochastic properties of the relevant collective variables. Note that D scales with $1/N^{1/2}$, which reflects the well-known effect of exchange narrowing of uncorrelated disorder.[28,29]

To end this section, we discuss the criteria for validity of the three-level approximation. The most important couplings which we neglected are the ones to the $k = \pm 2$ subspace, as this pair is closest in energy to the selected subspace. In particular, the dominant deformation-induced coupling which we omitted is the one between $|k = 0\rangle$ and $|k = \pm 2\rangle$ (the one between $|x\rangle$ or $|y\rangle$ and $|k = \pm 2\rangle$ vanishes), giving as criterion

$$\alpha \ll |E_{k=2} - E_{k=0}| \tag{21}$$

with E_k as defined in eq 9. On the other hand, the most important disorder-induced coupling which we neglected is the one between $|x\rangle$ (the highest state in our subspace if we assume that $\alpha > 0$, see Figure 2) and $|k = \pm 2\rangle$, and is typically given by $(\langle|\langle k = \pm 2|H_{dis}|x\rangle|^2\rangle)^{1/2} \approx D$. Thus, the criterion for neglecting the coupling due to disorder reads

$$D \ll |E_{k=2} - E_{k=1} - \alpha| \tag{22}$$

III. Diagonalization and Splitting Distribution

The analytical diagonalization of H_{red} as given in eq 13 and the determination of the statistics of its eigenvalues and

eigenvectors is still too difficult a task. Motivated by the observations in ref 6, we therefore at first further reduce the problem to a two-level one by neglecting the couplings V_x and V_y. We will return to the three-level reduction in section IV. Obviously, the two-level reduction is only meaningful if

$$D \ll |\delta - \alpha| \tag{23}$$

(cf. eq 20). The validity of this condition is facilitated by the factor $1/N^{1/2}$ occurring in D. Under this condition, the only two optically active eigenstates are given by

$$|+\rangle = \cos\Theta|x\rangle + \sin\Theta|y\rangle \tag{24}$$

$$|-\rangle = \sin\Theta|x\rangle - \cos\Theta|y\rangle \tag{25}$$

with $\tan\Theta = (-\Delta - \alpha + [(\Delta + \alpha)^2 + V^2]^{1/2})/V$. The energies of these states are given by

$$E_{\pm} = \delta + h \pm \sqrt{(\Delta + \alpha)^2 + V^2} \tag{26}$$

Thus, the spectrum for a single ring is given by two peaks, which are centered at the energies $E_{\pm}$ and have a width given by the homogeneous line width of the exciton transitions. Assuming that the molecular dipole orientations maintain the circular symmetry of the undistorted ring, the two peaks are polarized perpendicular to each other and have equal oscillator strength. The direction of polarization and the positions of the peaks are dictated by the particular realization of the deformation and the disorder and thus vary from ring to ring. The joint distribution function for h, Δ, and V, which from section II is found to take the form

$$P(h,\Delta,V) = \frac{2}{(2\pi)^{3/2}D^3}\exp\left(-\frac{\Delta^2 + V^2}{D^2}\right)\exp\left(-\frac{h^2}{2D^2}\right) \tag{27}$$

in principle allows one to determine the distribution functions of all these spectral properties. This fact may be used in two ways. First, $P(h,\Delta,V)$ may be used to calculate the ensemble-averaged absorption spectrum, obtained in conventional absorption experiments. Second, and more interestingly, the distribution functions derived from $P(h,\Delta,V)$ can be compared directly to distribution functions that may be obtained from single-aggregate experiments. Here, we will focus on the positions of the two peaks in the spectrum, which for a single ring are positioned symmetrically around $\bar{H} = \delta + h$ and are separated by

$$E \equiv 2\sqrt{(\Delta + \alpha)^2 + V^2} \tag{28}$$

From single-ring experiments, the mean position $\bar{H}$ and the separation E between the peaks can be measured, so that the joint probability distribution $P(\bar{H},E)$ for these two quantities can be obtained. It is obvious from eqs 27 and 28 that $\bar{H}$ and E are uncorrelated

$$P(\bar{H},E) = P(\bar{H})P(E) \tag{29}$$

with

$$P(\bar{H}) = \frac{1}{\sqrt{2\pi}D}\exp\left(-\frac{(\bar{H} - \delta)^2}{2D^2}\right) \tag{30}$$

In the remainder of this section we will concentrate on the calculation of $P(E)$. Formally, it is given by

$$P(E) = \int_{-\infty}^{+\infty} d\Delta \int_{-\infty}^{+\infty} dV \frac{1}{\pi D^2}\left(-\frac{\Delta^2 + V^2}{D^2}\right)\delta(E - 2\sqrt{(\Delta + \alpha)^2 + V^2}) \tag{31}$$

where we used the distribution function for Δ and V as extracted from eq 27. We now introduce ρ and φ such that $\Delta = -\alpha + \rho\cos\varphi$ and $V = \rho\sin\varphi$, which leads to

$$P(E) = \frac{1}{\pi D^2}\int_0^{2\pi} d\varphi \int_0^{\infty} d\rho\, \rho \exp\left(-\frac{\rho^2 + \alpha^2 - 2\alpha\rho\cos\varphi}{D^2}\right)\delta(E - 2\rho) \tag{32}$$

Owing to the δ function, the ρ integration may now be performed, leaving as φ integral one of the representations of the modified Bessel function of the first kind, $I_0(z)$.[30] The final result reads

$$P(E) = \frac{E}{2D^2}\exp\left(-\frac{(E/2)^2 + \alpha^2}{D^2}\right) I_0\left(\frac{|\alpha|E}{D^2}\right) \tag{33}$$

In Figure 3, $P(E)$ is plotted for several values of $|\alpha|/D$. In general, the distribution is strongly asymmetric with respect to its maximum. Its width is determined by D, while the position of the maximum and the average are determined by both D and α. In the limit of small deformation ($|\alpha| \ll D$), the distribution function reduces to

$$P(E) = \frac{E}{2D^2}\exp\left(-\frac{E^2}{4D^2}\right)\left(1 - \frac{\alpha^2}{D^2}\left[1 - \frac{E^2}{4D^2}\right] + ...\right) \tag{34}$$

In particular, in the limit of $\alpha = 0$, the distribution agrees with the standard result for Gaussian orthogonal ensembles of 2×2 matrices (Wigner surmise).[31,32] On the other hand, in the limit of small disorder ($D \ll |\alpha|$), the distribution reduces to

$$P(E) = \frac{1}{\sqrt{4\pi}D}\left(-\frac{(E - 2|\alpha|)^2}{4D^2}\right)\sqrt{\frac{E}{2|\alpha|}}\left(1 + \frac{D^2}{8|\alpha|E}\right) \tag{35}$$

which holds everywhere except for small energies ($E < D^2/|\alpha|$). The distribution eq 35 is a skewed Gaussian, with its maximum close to $E = 2|\alpha|$ and standard deviation approximately $\sqrt{2}D$. In the extreme limit of vanishing disorder ($D = 0$), the distribution reduces to $\delta(E - 2|\alpha|)$.

IV. Application to LH2

We will now use the results of section III to analyze the experiments on the B850 ring of the bacterial LH2 complex performed by van Oijen et al.[6,33] The B850 ring contains 18 bacteriochlorphyll molecules and has an exciton bandwidth in the order of 1200 cm^{-1}. In the experiments of ref 6, 17 different single-LH2 systems were studied, whose excitation spectra in the B850 region were typically dominated by two peaks of perpendicular polarization (see section I). Like Van Oijen et al., we will interpret these two lines as resulting from a disorder- and deformation-induced mixing in the $k = \pm 1$ subspace, as studied in the previous section. Thus, the experiments yield for each complex the average position $\bar{H} = \delta + h$ of the two peaks and their spectral separation E. Experimentally, both quantities are found to vary from complex to complex, while no clear correlation between $\bar{H}$ and E is observed.[33] The latter is in agreement with the factorization of $P(\bar{H},E)$ as in eq 29.

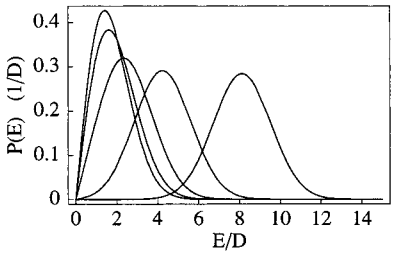

Figure 3. Distribution of energy splittings $P(E)$ according to eq 33 for $|\alpha|/D = 0.1$, 0.5, 1.0, 2.0, and 4.0 when moving from left to right in the figure.

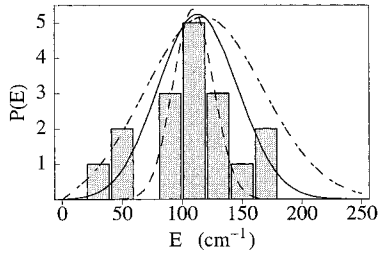

Figure 4. Histogram for the experimentally observed energy splitting E in the B850 ring of single LH2 complexes (ref 6), compared to our analytical result eq 33 for three different values of the effective disorder strength: $D = 12$ cm^{-1} (dashed), $D = 24$ cm^{-1} (solid), and $D = 36$ cm^{-1} (dash−dotted). In all three cases, we have taken $\alpha = 54$ cm^{-1}.

Figure 4 shows the histogram reported in ref 6 for the splitting E. In the same figure, we also plot our analytical result eq 33 for the three effective disorder strengths $D = 12$ cm^{-1}, $D = 24$ cm^{-1}, and $D = 36$ cm^{-1}, while we always take $\alpha = 54$ cm^{-1}. For the case of an elliptical deformation as described in the Appendix (ignoring contributions from α_1), $\alpha = 54$ cm^{-1} corresponds to an eccentricity $e = 0.50$ (from eq A14 with[16,34] $\gamma = 20°$ and $J = -282$ cm^{-1}). If we consider the longitudinal phonon distortion, the amplitude which corresponds to $\alpha = 54$ cm^{-1} is given by $Q/R = 0.032$ (from eq A8). We note that the parameter set $\alpha = 54$ cm^{-1} and $D = 12$ cm^{-1} is practically identical to the one used in the complete simulation in ref 6, where an ellipsoidal deformation with an eccentricity of $e = 0.52$ was used, while the effective disorder strength was $D \approx 12.5$ cm^{-1} ($\sigma \approx 53$ cm^{-1} (fwhm 125 cm^{-1}), and $\tau = 0$). Indeed, our analytical result for this parameter set agrees well with the results of the full 18-level simulation of ref 6, suggesting that for this disorder strength our two-level reduction is quite accurate.

We note that for the above relatively small D/α ratios the position of the maximum of the distribution $P(E)$ is mainly determined by the deformation alone and is hardly affected by the disorder strength. This makes a rather accurate determination of α possible. The disorder strength only has a strong effect on the width of the distribution, which experimentally, unfortunately, is not very well defined yet due to the still rather poor statistics. Consequently, it is hard to judge from Figure 4 what is the best fit to the experimental histogram, but it seems that $D = 12$ cm^{-1} is a very conservative estimate. We therefore rather opt for $D = 24$ cm^{-1}.

We now turn to the distribution $P(\bar{H})$ for the mean position of the two main absorption peaks in each complex. Figure 5 displays the histogram of experimentally observed values for $\bar{H}$,[33] where the zero of energy has been shifted to 11 626.4 cm^{-1} which is the average of $\bar{H}$ taken over all 17 complexes. According to eq 30, this distribution should be a Gaussian of standard deviation D. The solid curves in Figure 5 represent this Gaussian for the disorder strengths $D = 12$, 24, and 36 cm^{-1}. Again, the rather poor statistics makes it hard to fit the histogram to a Gaussian, but it can clearly be deduced that the value of $D = 24$ cm^{-1}, adopted as best choice to fit $P(E)$, gives a much too small width for $P(\bar{H})$. Even $D = 36$ cm^{-1} gives a width that is too small. Thus, it seems impossible to fit both $P(E)$ and $P(\bar{H})$ with the same parameter set.

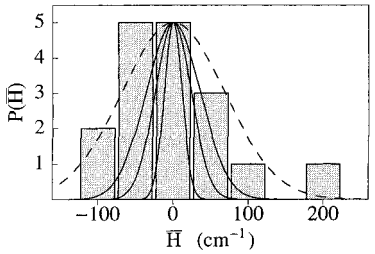

Figure 5. Histogram for the experimentally observed average position of the two peaks which dominate the absorption spectra of the B850 ring of single LH2 complexes,[33] compared to the Gaussian eq 30 for (with increasing width) $D = 12$ cm^{-1}, $D = 24$ cm^{-1}, and $D = 36$ cm^{-1} (solid curves). The dashed curve gives the theoretical distribution obtained for $D = 24$ cm^{-1} and an extra inter-ring disorder component with standard deviation $\sigma_{\text{inter}} = 64$ cm^{-1}. The zero of the horizontal scale corresponds to 11 626.4 cm^{-1} (see text).

A possible solution to this problem lies in the occurrence of not only intra-ring disorder, but also inter-ring disorder, a situation that has been considered before in the context of photon echo studies of molecular J-aggregates.[35] The general idea of the distinction between these two types of disorder is as follows. In our model, we have assumed that the random quantities ϵ_n and j_n have mean values that are equal for all molecules and bonds in all complexes. Due to heterogeneities in the sample at macroscopic length scales (or length scales much larger than a complex), it may be, however, that these mean values differ from ring to ring. This introduces disorder between rings, which can never be described by a distribution within a single ring. Other sources of such inter-ring disorder could be a variation of the deformation amplitude or wavelength, of relaxation rates, etc. For explicitness, we will restrict ourselves to inter-ring disorder in the site energies. We thus write the transition energy of the nth molecule in the Mth complex as

$$\epsilon_{Mn} = \epsilon_M + \epsilon_n(M) \tag{36}$$

where ϵ_M is taken from a Gaussian with mean zero and standard deviation σ_{inter}, while the $\epsilon_n(M)$ are taken from a Gaussian distribution with mean zero and standard deviation σ. The case $\sigma_{\text{inter}} = 0$ corresponds to the situation considered thus far, where the expectation value of the molecular transition energies in each complex is equal. By allowing for the case $\sigma_{\text{inter}} \neq 0$, we account for macroscopic inhomogeneity; an alternative way of modeling such effects is to assume finite correlations in the molecular disorder.[28,29] From the ensemble-averaged absorption spectrum, it is hard to distinguish between contributions from σ and σ_{inter}. It takes nonlinear optical techniques, like pump−probe[29,36] or photon echo[35,37,38] experiments, to make such a distinction for an ensemble. Single-aggregate absorption spectra offer an interesting and very direct alternative. Clearly, the energy splitting E is not affected by adding the inter-ring disorder, as it does not change the energy differences within a complex. Thus, $P(E)$ is still given by eq 33. On the other hand, the distribution of the average position $\bar{H}$ now changes its width (standard deviation) to

$$\sigma_{\text{total}} = \sqrt{D^2 + \sigma_{\text{inter}}^2} \tag{37}$$

($D = \sigma/N^{1/2}$). Thus, the inconsistency between the fits of $P(E)$ and $P(\bar{H})$ may be solved by assuming that $P(\bar{H})$ contains an appreciable extra broadening due to macroscopic inhomogeneity in the sample. Accepting for σ_{total} the standard deviation of the experimentally observed set of $\bar{H}$ values ($\sigma_{\text{total}} \approx 68$ cm^{-1})[33] and taking $D = 24$ cm^{-1} as best fit to the $P(E)$ histogram, we arrive at $\sigma_{\text{inter}} \approx 64$ cm^{-1}. The corresponding distribution for $\bar{H}$ is shown in Figure 5 as dashed curve. As σ_{inter} is not exchange narrowed, its effect on the ensemble-averaged absorption spectrum is much larger than the effect of the intra-ring disorder σ. We finally note that the inclusion of inter-ring disorder does not affect the validity criteria for the few-level reduction.

We now turn to a discussion of the criteria eqs 21 and 23 for the two-level reduction. To this end, we need the energy separations $E_{k=1} - E_{k=0}$ and $E_{k=2} - E_{k=1}$ at the bottom of the unperturbed exciton band. This requires knowledge of transfer interactions, $J_{n,m}$, which introduces some uncertainties. For the nearest-neighbor interaction, one generally agrees on a strength of about -300 cm^{-1}. Recent ab initio calculations have confirmed this value.[11] For the relevant energy separations, however, it is important to include interactions beyond the nearest-neighbor one, which are known with less accuracy. We will follow ref 16 and use the coupling set $J_0 \equiv J_{n,n\pm1} = -282$ cm^{-1}, $J_{n,n\pm2} = -43$ cm^{-1}, and $J_{n,n\pm3} = -12$ cm^{-1}. All longer-range interactions are negligibly small. The choice of sign of the interactions is consistent with the choice of the dipole directions in Figure 1 (other signs are obtained if the dipoles are alternatingly reversed in direction).[16] We have ignored the small dimerization in the ring, which gives rise to an alternation in the above interactions,[10,11,16] as well as in the site energies.[10] One easily shows that this alternation may be neglected for our purpose.

Using the above numbers in eq 9, one finds $E_{k=2} - E_{k=1} = 239$ cm^{-1}, implying that the criterion eq 21 is easily obeyed for $\alpha = 54$ cm^{-1}, as obtained from our analyis. For $\delta = E_{k=1} - E_{k=0}$, we find a value of 66 cm^{-1}, which would imply that the criterion eq 23 is not obeyed for the obtained parameters. Instead, one should expect that the $k = 0$ state strongly mixes with the states $|x\rangle$ and $|y\rangle$. Yet, the single-LH2 experiments revealing two perpendicularly polarized absorption peaks[6] strongly suggest the two-level picture and seem to exclude such mixing. As possible solutions to this paradox, we first note that the value of δ is uncertain, as a result of the uncertainty in the interactions. In fact, in refs 16 and 39, a level separation of $\delta = 90-100$ cm^{-1} is suggested, which would considerably improve the consistency of our two-level analysis. In ref 6, Van Oijen et al. note that they have also been able to identify the $k = 0$ state in a few complexes. Unfortunately, they do not report the position of this state relative to the main absorption peaks, but their Figure 3B suggests a value of $\delta \approx 100$ cm^{-1} for that particular complex. While stressing the obvious lack of statistical meaning of this number, we note that this does agree with the above numbers. At the same time, it should be noted that for this value of δ and for $D = 12-24$ cm^{-1}, one expects (from straightforward numerical simulations) that on the average 3.5−10% of the total oscillator strength resides in the $k = 0$ state. This means that one should expect this state to be clearly observable if one is able to compensate for the effect of spectral diffusion on this narrow lowest-energy line.

Next, we should point out that the experimental observations may in fact also be consistent with a strong mixing of the $k = 0$ state into the $k = \pm1$ subspace. This becomes clear if we reconsider the three-level Hamiltonian eq 13. Since the value of α suggested by the above analysis is very close to the calculated value of δ (66 cm^{-1}), we may have a situation where the states $|k = 0\rangle$ and $|y\rangle$ happen to be almost resonant with each other, leading to their strong mixing by disorder. In fact, if $D \ll \sqrt{2}\alpha$ and at the same time D is of the same order as or larger than $|\delta - \alpha|$, the states $|k = 0\rangle$ and $|y\rangle$ will strongly mix, while these states may be considered decoupled from the third state $|x\rangle$ (for explicitness, we again assumed $\alpha > 0$). This situation may be considered the alternative limit to our two-level approximation of section III.

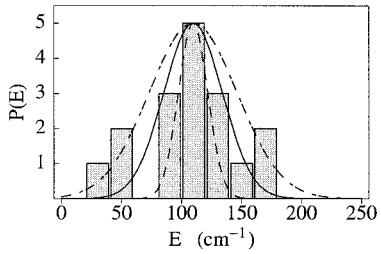

Figure 6. Histogram for the experimentally observed energy splitting E in the B850 ring of single LH2 complexes (ref 6), compared to our anayltical result in the case of strong coupling between the two states $|k = 0\rangle$ and $|y\rangle$. The theoretical curves correspond to a disorder strength of $D = 12$ cm^{-1} (dashed), $D = 24$ cm^{-1} (solid), and $D = 36$ cm^{-1} (dash−dotted). In all three cases, we have taken $\alpha = 51$ cm^{-1}.

Under these conditions, each ring will have one absorption peak associated with the state $|x\rangle$, at the energy $E_+ = \delta + h + \alpha + \Delta$. Furthermore, the mixing of the two other states in principle gives rise to two more absorption peaks, which both have polarization perpendicular to the $|x\rangle$ state. Clearly, the occurrence of two lowest absorption peaks with identical polarization is hard to reconcile with the experimental observations. If, however, these two peaks have a homogeneous width that is comparable to or larger than their distance (which typically is D), the two lower states appear as one peak in the experiment, and one recovers a single-ring absorption spectrum that is dominated by two perpendicularly polarized absorption peaks. In this situation, the center of the low-energy peak lies at $E_- = h + (\delta - \alpha - \Delta)/2$. Thus, the average position of the two observed absorption peaks in this limit is given by

$$\bar{H} = \frac{3\delta + \alpha}{4} + h + \frac{\Delta}{4} \tag{38}$$

$$E = \frac{\delta + 3\alpha}{2} + \frac{3\Delta}{2} \tag{39}$$

Clearly, in contrast to the two-level approximation, we now do find a finite correlation between $\bar{H}$ and E, which, however, is rather weak and cannot be excluded on the basis of the experiments. The marginal distribution for $\bar{H}$ resulting from eq 38 is a Gaussian with a standard deviation of $(33/32)^{1/2}D$, while the distribution for E as in eq 39 is a Gaussian with a standard deviation of $3D/\sqrt{8}$. Note that these widths are almost equal to each other.

Figure 6 shows the comparison of the thus obtained distribution $P(E)$ for $D = 12$, 24, and 36 cm^{-1}, with $\alpha = 51$ cm^{-1} to experiment. It appears that in this limit of the theory, an effective disorder strength in the order of $D = 30$ cm^{-1} covers the experiment best. Similarly to our earlier findings, however, this disorder strength clearly is too small to fit the width of the experimentally observed distribution for $\bar{H}$ ($\sigma_{\text{total}} \approx 68$ cm^{-1}). The discrepancy can again be solved by assuming appreciable inter-ring disorder, which for $D = 30$ cm^{-1} should amount to $\sigma_{\text{inter}} \approx 61$ cm^{-1}. We thus find that the conclusion concerning

the presence of inter-ring disorder is hardly affected by the strong mixing of the $k = 0$ state with the $k = \pm 1$ subspace. We finally note that the homogeneous line width reported for the exciton lines in ref 6 is in the order of 50 cm^{-1}, which is indeed larger than D and thus is consistent with the assumption made above.

V. Concluding Remarks

In this paper, we have derived analytical results for the statistics of the absorption spectra of individual ring-shaped molecular aggregates with static energy and interaction disorder and a ring distortion. Our results are based on a reduction of the Hamiltonian to a few (2 or 3) relevant exciton states. Analytical results could be obtained, because the disorder enters the effective few-level Hamiltonian eq 13 through five *uncorrelated* collective stochastic variables. The latter are all characterized by one collective disorder strength D, which is an exchange-narrowed combination of the underlying energy and interaction disorder strengths (σ and τ, respectively, cf. eq 19). The validity of the few-level reduction is governed by three parameters: the level separation δ at the bottom of the unperturbed exciton band, the deformation-induced splitting 2α, and the effective disorder strength D. Generally, the smaller the ratios D/δ and α/δ, the better the reduction.

Using our results, we have analyzed the fluorescence excitation experiments on the B850 ring of single LH2 complexes of the bacterial photosynthetic system.[6,33] We have shown that if we focus on the two perpendicularly polarized low-energy peaks that dominate these spectra, we arrive at values for D and α that justify a three-level ($k = 0, \pm 1$ subspace) approach, while the reduction to the two-level ($k = \pm 1$) subspace, as was strongly suggested in ref 6, sensitively depends on the precise value for δ. Interestingly, the typical paramaters obtained from our analysis do not depend very much on whether the two-level or strongly coupled three-level case is applicable. With due error bars in view of the poor experimental statistics, our analysis indicates $D \approx 24-30$ cm^{-1} and $\alpha \approx 50$ cm^{-1}. Moreover, our analysis shows that a consistent understanding of both the observed splitting distribution and the fluctuations in the mean positions of the observed absorption peaks is only possible if we account for an appreciable inter-ring disorder (macroscopic inhomogeneity) $\sigma_{inter} \approx 64$ cm^{-1}. The obtained value for D is equivalent to a molecular diagonal disorder strength of the order of $\sigma \approx 100$ cm^{-1} (assuming absence of interaction disorder). The value for α corresponds to ring deformations of the order of 3−15% of the radius, depending on the type of deformation one considers. In fact, we point out that the modulation of the transfer interactions described by α may also originate from a different source than a ring deformation, e.g., from an anisotropy in the interactions originating from an anisotropic dielectric constant of the host medium.

In our model, we have assumed the deformation to be static, i.e., it already exists in the electronic ground state. In principle it may also be of dynamic nature: the two Bloch states $|k = \pm 1\rangle$ are degenerate in the absence of disorder and thus give rise to a Jahn−Teller distortion in the electronically excited state. This spontaneously generated distortion results in two electronic terms, similarly to the level-splitting in the case of static distortion (Figure 2). In ref 6 the relevance of this effect for the explanation of the observed two-peak absorption spectra was ruled out on the basis of the fact that the necessary value for α would be unrealistically large. We stress, however, that the Jahn−Teller effect even in principle cannot explain the occurrence of two peaks with perpendicular polarization in the single-ring spectrum. The reason is that, due to the axial symmetry of the two electronic terms in the two-dimensional space of nuclear coordinates describing the ellipsoidal deformation, each of the electronic terms has a doubly degenerate nuclear ground state. This degeneracy exactly renders the two peaks associated with the two electronic terms unpolarized. We note that this is a rigorous statement, which is independent of the effective mass of the phonon mode involved in the distortion. It thus also holds for a small effective mass, where a transition between the undistorted ground state and a distorted excited state is possible due to quantum lattice fluctuations.

Returning to static deformations, we note that a few-level reduction, as we have used, necessarily excludes strong localization of the excitons on only a few molecules. Delocalization over almost the full ring was, in fact, one of the main conclusions of ref 6. As noted in the Introduction, however, values for the exciton delocalization length obtained in various types of experiments differ widely. While it is not the main goal of this paper to determine the delocalization length, it seems worthwhile to comment briefly on this quantity. First, it should be stressed that different experimental techniques are sensitive to different moments of the wave functions and, thus, may differ in the length that they attribute to the exciton. In addition, also the theoretical definition of the delocalization length is not unique (participation ratio, autocorrelation of the wave function, decay of the wave function tails, etc). In large systems, these measures give comparable length scales, but they may differ in their exact size. In small systems of only 18 molecules, this difference only makes it meaningful to distinguish between strong (almost the complete ring) and weak (a few molecules) delocalization. Second, one should distinguish between the delocalization length imposed on the wave function by static disorder, which is relevant at low temperatures, and the coherence length, which is also influenced by scattering on dynamic degrees of freedom.[19] The latter is (unfortunately) also often referred to as delocalization length and is temperature dependent.[40] In this sense, low-temperature experiments generally measure larger "delocalization sizes" than high-temperature ones. The experiments in ref 6 have been performed at 1.2 K, where one expects dynamic effects to be small. This seems in strong contradiction with superradiance experiments,[17] which even at 4 K give a superradiant enhancement of only 2−3, suggesting a small delocalization size. It was recently shown, however, that these data can also be reconciled with small disorder and a strong delocalization.[23] Third, the time scale of the experiment may be of relevance, as longer time scales make it possible for the initially excited exciton(s) to relax to a lower lying and more localized exciton state. Such relaxation has been monitored in two-color femtosecond absorption spectroscopy.[41] The pump−probe experiments in ref 18, which gave a temperature-independent delocalization size of roughly four molecules, had a waiting time of 1.5 ps, which does allow for relaxation. Finally, we note that almost all experiments have thus far been performed on ensembles of complexes. We stress, however, that the ensemble avaraging may hide some of the underlying properties of individual rings and may lead to an underestimation of the delocalization size in single rings.

To illustrate the latter point, we consider the example of the exciton delocalization length as determined from the width of the ensemble averaged absorption peak.[24] This length lies in the range of 6−9 molecules, depending on the value one accepts for the homogeneous line width of the exciton transitions. As we pointed out in ref 24, however, the existence of inter-ring disorder may give rise to an underestimation of the delocaliza-

tion length through this method. The reason is that such disorder does not affect the delocalization length on a single ring, while it does broaden the ensemble-averaged absorption line. As we have seen in the present paper, the single-complex experiments suggest a rather large strength of the inter-ring disorder (at least in the samples of ref 6). In fact, if we correct the low-temperature ensemble absorption spectrum[39] for this inter-ring disorder by deconvoluting with the Gaussian of width $\sigma_{\text{inter}} \approx 64\ \text{cm}^{-1}$, the delocalization length estimated from the absorption spectrum at low-temperature grows to 12 molecules, consistent with delocalization over a substantial part of the ring. Similarly, inter-ring disorder leads to underestimating the delocalization length obtained from the transient absorption spectrum,[42,43] as it has an analogous effect as the inclusion of an extra homogeneous line width to the exciton transitions.[43]

The direct insight into the delocalization length and the inter-ring disorder demonstrate the potential power of single-aggregate experiments. It should be noted, however, that for several LH2 complexes observed, the experimental data[6,33] reveal features that are hard to reconcile with the current model, even if we account for a wider range of parameters. Several rings clearly show a third and sometimes even a fourth peak in the fluorescence excitation spectrum. These peaks occur at higher energies and always are of lower intensity than the dominant peaks. Even in the presence of these extra peaks, the dominant peaks maintain their property of perpendicular polarization.[33] The polarization of the additional peaks seems to be correlated with that of the dominant peaks, although the lack of statistics renders this observation rather uncertain. We have considered several possible explanations for these extra peaks. (i) The obvious first choice would be that one in fact observes three or four separated states that result from a strong mixing of the lowest Bloch states by disorder. This picture is inconsistent, however, with the observed polarization properties of the peaks. (ii) The extra peaks derive from the fact that the $k = \pm 3$ states acquire oscillator strength due to the deformation-induced coupling to the $k = \pm 1$ states. This seems to be a very good possibility, as these states indeed are directly coupled by the deformation of wave vector 2ϕ. Also the typical energy separation of $\delta'' \approx 300-400\ \text{cm}^{-1}$ [6] between the extra peaks and the dominant low-energy ones seems to be consistent with this interpretation. Simple estimates, however, show that no consistent choice can be made for the exciton−phonon coupling α that simultaneously explains the separation between the two dominant peaks and the intensity in the extra peak(s) (the latter is dominated by $|\alpha/\delta''|^2$). (iii) Finally, we have considered the possibility that due to the ring deformation and a concomitant possible reorientation of the molecular transition dipoles along the local tangent of the ellipse, the $k = \pm 3$ states become optically allowed, even if we disregard mixing to the $k = \pm 1$ states. This effect is dominated by $|\alpha/J_0|^2$ and, again, seems to be much too small to explain the observed intensities in the extra peak(s).

We conclude that the above observations call for further studies. Experimentally, the focus should be on considerably extending the statistics of the single-molecule experiments. Here, special attention should be paid to the polarization of the two dominant peaks, to the position, polarization, and oscillator strength of the highler lying (additional) peaks, to the position, polarization, and oscillator strength of the "$k = 0$" state, and to the possibility to detect the upper band edge of the B850 band (for instance by using genetically modified complexes, in which the B800 ring is absent). All these data should give more insight into the actual bandwidth, the values of δ and δ', and the interpretation of the additional peaks (are they typical or exceptional?). More statistics would make a fit of observed distribution functions to the theory presented here more meaningful, leading to a more stringent test of the model we presented. In addition, better statistics would make a determination of correlation functions and their comparison to theory possible. Such correlations can also involve other measured quantities, such as the oscillator strengths. Interpreting these correlations would involve further theoretical analysis, which can probably only be carried out by numerical simulations. Finally, on the theoretical side, in order to translate the value for α into better founded deformation amplitudes, it will be necessary to develop more detailed models describing the relevant intermolecular interactions.

Note Added in Proof. We have recently learned that the analytical analysis of the experiments in ref 6 which we have reported here, is confirmed by numerical simulations by Ketelaars et al.[44] If we translate the parameters which these authors use to our notation, they find a best fit for $D = 25\ \text{cm}^{-1}$, a ring deformation of 8.5%, while they also conclude that considerable inter-ring disorder exists ($\sigma_{inter} = 51\ \text{cm}^{-1}$). These numbers agree well with our analytical results and confirm the accuracy and relevance of the few-level theory presented here. In addition, the authors of ref 44 also report a more detailed analysis of the available experimental data concerning the $k = 0$ state and they conclude that this state has an oscillator strength of 2−9% of the total oscillator strength in the B850 band. This agrees well with our estimate of 3.5−10%. The numerical approach also indicates that a relatively small disorder in the deformation amplitude may in fact explain the occurrence of rather strong higher-energy peaks for some rings.[44]

Acknowledgment. We are grateful to Prof. Dr. J. Schmidt, Prof. Dr. T. J. Aartsma, and Prof. Dr. J. Köhler for many stimulating discussions and for sharing several of their experimental results with us prior to publication. We also acknowledge helpful discussions with Prof. R. van Grondelle. This work is part of the research program of the Stichting voor Fundamenteel Onderzoek der Materie (FOM), which is financially supported by the Nederlandse Organisatie voor Wetenschappelijk Onderzoek (NWO).

Appendix A: Two Specific Deformation Models

In this Appendix, we calculate α_2, the depth of the interaction modulation, arising from two types of deformations of the original ring system. We will assume that the transfer interactions are mediated through the transition point dipoles:

$$J_{nm} = \frac{1}{x_{nm}^3}[(\mathbf{d}_n \cdot \mathbf{d}_m) - 3(\mathbf{d}_n \cdot \hat{\mathbf{x}}_{nm})(\mathbf{d}_m \cdot \hat{\mathbf{x}}_{nm})] \qquad \text{(A1)}$$

Here, $\mathbf{d}_n$ is the transition dipole of molecule n, while $\mathbf{x}_{nm} = x_{nm}\hat{\mathbf{x}}_{nm} = \mathbf{x}_n - \mathbf{x}_m$, with $\mathbf{x}_n$ the position of molecule n. If the geometry of the ring is distorted such that $\mathbf{x}_n \rightarrow \mathbf{x}_n + \delta\mathbf{x}_n$, the change of interaction to first order in this distortion is given by

$$\delta J_{nm} = -3\frac{d_n^\mu d_m^\nu \delta x_{nm}^\sigma}{x_{nm}^4}[\delta^{\mu\nu}\hat{x}_{nm}^\sigma + \delta^{\nu\sigma}\hat{x}_{nm}^\mu + \delta^{\sigma\mu}\hat{x}_{nm}^\nu - 5\hat{x}_{nm}^\mu \hat{x}_{nm}^\nu \hat{x}_{nm}^\sigma] \qquad \text{(A2)}$$

where μ, ν, and σ indicate Cartesian components, the summation over which is implicit. We assumed that the dipoles are not

affected in magnitude or orientation by the distortion. In particular, we will assume that the dipole of molecule n makes an angle $\pi/2 + \gamma$ with the position vector $\mathbf{x}_n = (R \cos n\phi, R \sin n\phi)$ which this molecule has in the undistorted ring (Figure 1). We will only account for the change $\delta J_{n,n+1}$ in the nearest-neighbor interactions due to the distortion.

In the first distortion model, the molecular positions can only shift along the ring, so that the distance of a molecule to the center of the ring remains R. Moreover, the deformation is assumed to have a plane-wave character with period $N/2$, i.e., with wavenumber $2\phi = 4\pi/N$. We thus have

$$\delta\mathbf{x}_n = \hat{\phi}_n Q \sin(2\phi n - \Phi') \tag{A3}$$

where $\hat{\phi}_n$ is the unit vector in the azimuthal direction at $\mathbf{x} = \mathbf{x}_n$, Q is the amplitude of the deformation, and Φ' is the phase. Straightforward algebra yields for the change of the dipole−dipole interactions due to this deformation:

$$\delta J_{n,n+1} = -\frac{6c_1 J_0 Q}{R} \cos\left(2\phi\left(n + \frac{1}{2}\right) - \Phi_2\right) \tag{A4}$$

with

$$c_1 = \left(\cos^4\frac{\phi}{2} + \frac{\cos^2\phi \sin^2 2\gamma}{(\cos\phi + 3\cos 2\gamma)^2}\right)^{1/2} \tag{A5}$$

Furthermore, J_0 indicates the nearest-neighbor coupling in the undistorted ring, given by

$$J_0 = -\frac{d^2}{2l^3}(\cos\phi + 3\cos 2\gamma) \tag{A6}$$

with $l = 2R \sin\phi/2$ the nearest-neighbor distance. Finally, $\Phi_2 = \Phi' + \theta_1$, where

$$\tan\theta_1 = \frac{\cos\phi \sin 2\gamma}{\cos^2\frac{\phi}{2}(\cos\phi + 3\cos 2\gamma)} \tag{A7}$$

Comparing eq A4 to eq 3, we find that for this type of deformation the coupling constant α_2 is given by

$$\alpha_2 = -\frac{6c_1 J_0 Q}{R} \tag{A8}$$

We next turn to the second type of deformation, for which we will assume that the circle is slightly distorted into an ellipse of small eccentricity. In particular, we will assume that the short axis of the ellipse is R, while the long axis is $R(1 + \epsilon)$, with $\epsilon \ll 1$. The orientation of the long axis is arbitrary. If the polar coordinates of molecule n on this ellipse are denoted as (r_n, ϕ_n), we have

$$r_n^2 = \frac{R^2}{1 - e^2\cos^2(\phi_n - \Phi'/2)} \tag{A9}$$

where e is the eccentricity of the ellipse, which is given by $e^2 = (2\epsilon + \epsilon^2)/(1 + \epsilon)^2$, while $\Phi'/2$ denotes the orientation of the long axis. Since $\epsilon \ll 1$, we also have $e^2 \ll 1$, so that we may approximate

$$r_n = R\left(1 + \frac{1}{2}e^2\cos^2(\phi_n - \Phi'/2)\right) \tag{A10}$$

We will assume that the molecular positions on the ellipse are such that $\phi_n = n2\pi/N = n\phi$; i.e., the position angles are the same as on the undistorted ring. From eq A10 it is seen that in the small-distortion limit, the ellipse corresponds to a modulation of the position radii with wavenumber 2ϕ. Thus, the modulation of the interactions indeed is expected to behave according to eq 3. More explicitly, if we substitute $\mathbf{x}_n = (R \cos n\phi, R \sin n\phi)$ and $\delta\mathbf{x}_n = (1/2)e^2 \cos^2(\phi_n - \Phi'/2)\mathbf{x}_n$ into eq A2, we obtain

$$\delta J_{n,n+1} = -\frac{3}{4}e^2 J_0\left[1 + c_2 \cos\left(2\phi\left(n + \frac{1}{2}\right) - \Phi_2\right)\right] \tag{A11}$$

with J_0 as defined in eq A6

$$c_2 = \left(\cos^2\phi + \frac{4\cos^4\frac{\phi}{2}\sin^2 2\gamma}{(\cos\phi + 3\cos 2\gamma)^2}\right)^{1/2} \tag{A12}$$

and $\Phi_2 = \Phi' + \theta_2$, with

$$\tan\theta_2 = \frac{2\cos^2\frac{\phi}{2}\sin 2\gamma}{\cos\phi(\cos\phi + 3\cos 2\gamma)} \tag{A13}$$

Comparing eq A11 to eq 3, we find that for the ellipsoidal deformation the coupling constant α_2 is given by

$$\alpha_2 = -\frac{3}{4}e^2 c_2 J_0 \tag{A14}$$

Equation A11 also contains a constant term $-(3/4)e^2 J_0$, which arises from the fact that the average distance between the molecules increases relative to the original ring geometry, so that the average interaction decreases. This constant term obviously does not affect the splitting between the two exciton states $|+\rangle$ and $|-\rangle$, and may be considered to be absorbed into the term $\bar{H}$.

References and Notes

(1) Moerner, W. E.; Orrit, M. *Science* **1999**, *283*, 1670.

(2) Basché, Th.; Moerner, W. E.; Orrit, M.; Wild, U. *Single Molecule Optical Detection, Imaging, and Spectroscopy*; Verlag-Chemie: Munich, Germany, 1999.

(3) Bopp, M. A.; Jia Y.; Li, L.; Cogdell, R. J.; Hochstrasser, R. M. *Proc. Natl. Acad. Sci. U.S.A.* **1997**, *94*, 10630.

(4) Bopp, M. A.; Sytnik, A.; Howard, T. D.; Cogdell, R. J.; Hochstrasser, R. M. *Proc. Natl. Acad. Sci. U.S.A.* **1999**, *96*, 11271

(5) Oijen, A. M. van; Ketelaars, M.; Köhler, J.; Aartsma, T. J.; Schmidt, J. *Chem. Phys.* **1999**, *247*, 53.

(6) Oijen, A. M. van; Ketelaars, M.; Köhler, J.; Aartsma, T. J.; Schmidt, J. *Science* **1999**, *285*, 400.

(7) Tietz, C.; Chekhlov, O.; Dräbenstedt, A.; Schuster, J.; Wachtrup, J. *J. Phys. Chem. B* **1999**, *103*, 6328.

(8) Hu, X.; Schulten, K. *Phys. Today* **1997**, *50*, 28; and references therein.

(9) McDermott, G.; Prince, S. M.; Freer, A. A.; HawthornthwaiteLawless, A. M.; Papiz, M. Z.; Cogdell, R. J.; Isaacs, N. W. *Nature* **1995**, *374*, 517.

(10) Koolhaas, M. H. C.; Frese, R. N.; Fowler, G. J. S.; Bibby, T. S.; Georgakopoulou, S.; van der Zwan, G.; Hunter, C. N.; van Grondelle R. N. *Biochemistry* **1998**, *37*, 4693.

(11) Scholes, G. D.; Gould, I. A.; Cogdell, R. J.; Fleming, G. R. *J. Phys. Chem. B* **1999**, *103*, 2543.

(12) Schreiber, M.; Toyozawa, Y. *J. Phys. Soc. Jpn.* **1982**, *51*, 1537.

(13) Fidder, H.; Knoester, J.; Wiersma, D. A. *J. Chem. Phys.* **1991**, *95*, 7880.

(14) Novoderezhkin, V. I.; Razjivin, A. P. *FEBS Lett.* **1995**, *368*, 370.

(15) Leupold, D.; Stiel, H.; Teuchner, K.; Nowak, F., Sandner, W.; Ücker, B.; Scheer, H. *Phys. Rev. Lett.* **1996**, *77*, 4675.

(16) Sauer, K.; Cogdell, R. J.; Prince, S. M.; Freer, A.; Isaacs, N. W.; Scheer, H. *Photochem. Photobiol.* **1996**, *64*, 564.

(17) Monshouwer, R.; Abrahamsson, M.; Mourik, F. van; Grondelle, R. van *J. Phys. Chem. B* **1997**, *101*, 7241.

(18) Chachisvilis, M.; Kühn, O.; Pullerits, T.; Sundström, V. *J. Phys. Chem. B* **1997**, *101*, 7275.
(19) Meier, T.; Chernyak, V.; Mukamel, S. *J. Phys. Chem. B* **1997**, *101*, 7332.
(20) Jimenez, R.; Mourik, F. van; Fleming, G. R. *J. Phys. Chem. B* **1997**, *101*, 7350.
(21) Wu, H.-M.; Small, G. J. *J. Phys. Chem. B* **1998**, *102*, 888.
(22) Kumble, R.; Hochstrasser, R. M. *J. Chem. Phys.* **1998**, *109*, 855.
(23) Zhao, Y.; Meier, T.; Zhang W. M.; Chernyak, V.; Mukamel, S. *J. Phys. Chem. B* **1999**, *103*, 3954.
(24) Bakalis, L. D.; Knoester, J. *J. Lumin.* **2000**, *87*−*89*, 66.
(25) Mukai, K.; Abe, S.; Sumi, H. *J. Lumin.* **2000**, *87*−*89*, 818.
(26) Davydov, A. S. *Theory of Molecular Excitons*; Plenum: New York, 1971.
(27) Agranovich, V. M.; Galanin, M. D. In *Electronic Excitation Energy Transfer in Condensed Matter*; Agranovich, V. M., Maradudin, A. A. Eds.; North-Holland: Amsterdam, 1982.
(28) Knapp, E. W. *J. Chem. Phys.* **1983**, *85*, 73.
(29) Knoester, J. *J. Chem. Phys.* **1993**, *99*, 8466.
(30) Abramowitz, M.; Stegun, I. A. *Handbook of Mathematical Functions*; Dover: New York, 1972.
(31) Bohr, A.; Mottelson, B. R. *Nuclear Structure*; Benjamin: New York, 1975; p 294.
(32) Mehta, M. L. *Random Matrices*; Academic Press: Boston, MA, 1991.
(33) Oijen, A. M. van; Ketelaars, M.; Köhler, J.; Aartsma, T. J.; Schmidt, J., private communication.
(34) Kennis, J. Exciton Coupling, Energy Transfer and Photochemical Conversion in Purple Photosynthetic Bacteria; Ph.D. Thesis, Leiden University, 1997; p. 18.
(35) Spano, F. C. *J. Phys. Chem.* **1992**, *96*, 2844.
(36) Durrant, J. R.; Knoester, J.; Wiersma, D. A. *Chem. Phys. Lett.* **1994**, *222*, 450.
(37) Root, L.; Skinner, J. L. *Phys. Rev. B* **1985**, *32*, 4111.
(38) Yang, M.; Fleming, G. R. *J. Chem. Phys.* **2000**, *113*, 2823.
(39) Reddy, N. R. S.; Picorel, R.; Small, G. J. *J. Phys. Chem.* **1992**, *96*, 6458.
(40) Ray, J.; Makri, N. *J. Phys. Chem. A* **1999**, *103*, 9417.
(41) Vulto, S. I. E.; Kennis, J. T. M.; Streltsov, A. M.; Amesz, J.; Aartsma, T. J. *J. Phys. Chem. B*, **1999**, *103*, 878.
(42) Juzeliūnas, G. *Z. Phys. D* **1988**, *8*, 379.
(43) Bakalis, L. D.; Knoester, J. *J. Phys. Chem. B* **1999**, *103*, 6620.
(44) Ketelaars, M.; van Oijen, A. M.; Matsushita, M.; Köhler, J.; Schmidt, J.; Aartsma, T. J. *Biophys. J.* (submitted).